CONSTRAINTS ON THE DEPTH OF MARTIAN MANTLE TRANSITION ZONE FROM TRIPLICATED WAVEFORMS. Q. Huang[1,2], N. C. Schmerr[1], S. D. King[3], A. Rivoldini[4], A.-C. Plesa[5], H. Samuel[6], D. Kim[1], R. R. Maguire[1], F. Karakostas[1,7], V. Lekić[1], M. Collinet[5], R. Myhill[8], D. Antonangeli[9], M. Drilleau[10], M. Bystricky[11], C. Bollinger[11], C. Michaut[12], T. Gudkova[13], J. C.E. Irving[8], B. Fernando[14], K. Leng[14], T. Nissen-Meyer[14], F. Bejina[11], E. Bozdag[2], C. Beghein[15], L. Waszek[16], N. C. Siersch[9], J.-R. Scholz[17], P. M. Davis[15], P. Lognonné[6], B. Pinot[10], R. Widmer-Schnidrig[18], M. P. Panning[19], S. E. Smrekar[19], T. Spohn[5], D. Giardini[20], W. B. Banerdt[19]; [1]University of Maryland, [2]Colorado School of Mines, [3]Virginia Tech, [4]Royal Observatory of Belgium, [5]Institute of Planetary Research, German Aerospace Center (DLR), [6]Université de Paris, Institut de Physique du Globe de Paris, [7]Istituto Nazionale di Geofisica e Vulcanologia, Sezione di Bologna, [8]University of Bristol, [9]Sorbonne Université, [10]Institut Supérieur de l'Aéronautique et de l'Espace SUPAERO, [11]Institut de Recherche en Astrophysique et Planétologie, Université Toulouse III Paul Sabatier, [12] Université de Lyon, [13]Schmidt Institute of Physics of the Earth RAS, [14]University of Oxford, [15]UCLA, [16]James Cook University, [17]Max Planck Institute for Solar System Research, [18]Black Forest Observatory, Stuttgart University, [19]JPL, [20]ETH Zurich

Introduction: The knowledge of the mantle structure of Mars, including its thermal and compositional state, shed light on the formation and evolution of the planet. Previous mantle composition models of Mars have been constructed using geochemical data from Martian meteorites [1–6] as well as orbital geophysical data [7]. Using these a priori models, a seismic discontinuity resulting from the mineral phase transition from olivine to its higher-pressure polymorphs, including wadsleyite and ringwoodite, is predicted to exist between 950-1150 km depth [8–10]. This boundary demarcates the top of the mantle transition zone (MTZ) in Mars, which is equivalent to the 410-km discontinuity on Earth. The depth of the post-olivine transition is correlated with the mantle temperature due to its positive Clapeyron slope [10–11]. The sharpness of this phase transition is also sensitive to the temperature, iron [12] and water content [13–14] of the mantle. Therefore, the depth and sharpness of the seismic discontinuity provide invaluable insight into the temperature and composition of Martian mantle.

Methodology: We used P and S triplications, which are reflected and refracted waves interacting with the top of the MTZ, to detect this discontinuity. Using the seismic data from NASA's InSight Mission [15], we identified multiple low-frequency and broadband events that are located between 60-85 degrees [16] which is the epicentral distance range to observe mantle triplications (Figure 1). We used a polarization filter [17] to enhance the signal-to-noise ratio of these events. We then aligned them on their first P- and S-arrivals and ordered them by epicentral distance. This event alignment reveals secondary phases that are consistent with the predicted travel-times of P and S triplications.

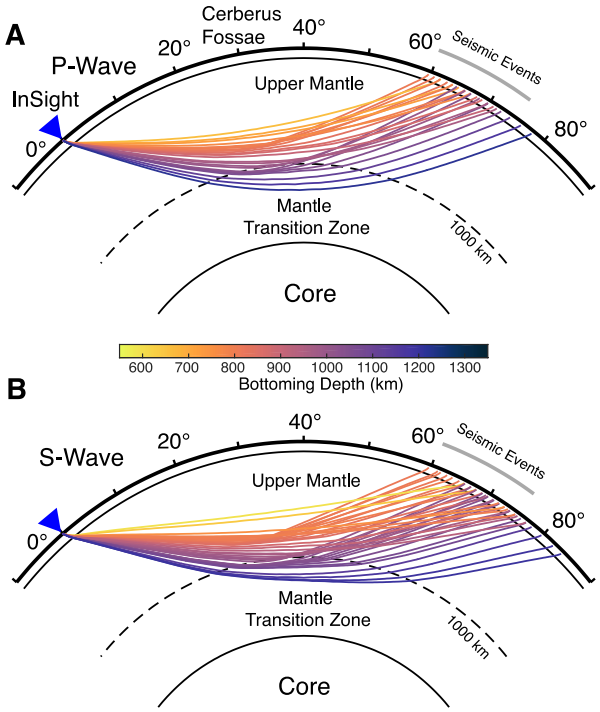

Figure 1. *Raypath geometry of mantle triplications in Mars. Teleseismic ray paths of (**A**) P-waves and (**B**) S-waves interacting with the discontinuity near the MTZ depth, colored according to their bottoming depths. The 1000-km discontinuity is associated with the post-olivine transition. Seismic velocity profile is based on a pre-landing model [18]. Triplications are formed between 60º - 85º from the InSight lander (blue triangle). Gray lines indicate the epicentral distances of the observed seismic events that show mantle triplications.*

We used a waveform modeling approach based on mineral physics models to fit the triplicated waveforms. To largely explore possible model space, we derived these mineral physics models from six

different composition models, covering the range of mantle potential temperature between 1305-1705 K, and satisfying the planet mass and moment inertia constraints. We then computed synthetic waveforms using the spectral element method AxiSEM [19] based on these mineral physics models. The synthetic waveforms were filtered and aligned with the data using a cross-correlation method. After the alignment, we computed the correlation coefficients to quantify the misfit between data and synthetics. We performed the waveform modeling for both P and S triplications to search for the models with minimum total misfits.

Results: From the waveform modeling, we find a suite of velocity models that can fit both the P and S triplications. The constrained range of MTZ depth indicates a Martian mantle with a potential temperature like Earth, but relatively colder than pre-mission estimates. Our results are consistent with the inversion of upper mantle structure from InSight data [20] as well as the geochemical analysis of Amazonian volcanic rocks [21]. We also find evidence for a broader post-olivine transition compared to the sharp 410-km discontinuity on Earth, confirming that Martian mantle is more iron-rich than Earth's mantle. Combined with the thermal evolution models [22, 23], we further explore the initial thermal state, mantle rheology and mantle composition of Mars based on the observed range of MTZ depth.

Acknowledgments: We acknowledge NASA, CNES, their partner agencies and Institutions (UKSA, SSO, DLR, JPL, IPGP-CNRS, ETHZ, IC, MPS-MPG) and the flight operations team at JPL, SISMOC, MSDS, IRIS-DMC and PDS for providing SEED SEIS data, and mission support. We acknowledge the funding from NASA grant 80NSSC18K1628.

References: [1] Dreibus, G. & Wänke, H. (1985) *Meteoritics* 20, 367–381. [2] Lodders, K. & Fegley, B. (1997) *Icarus* 126, 373–394. [3] Sanloup, C. et al. (1999) *Phys. of the Earth & Planet. Interiors* 112, 43–54. [4] Sohl, F. & Spohn, T (1997) *JGR Planets* 102, 1613–1635. [5] Taylor, G. J. (2013) *Chemie der Erde* 73, 401–420. [6] Yoshizaki, T. & McDonough, W. F. (2020) *Geochimica et Cosmochimica Acta* 273, 137–162. [7] Khan, A. *et al.* (2018) *JGR: Planets* 123, 575–611. [8] Bertka, C. M. & Fei, Y. (1997) *JGR: Solid Earth* 102, 5251–5264. [9] Ringwood, A. E (1975), *McGraw-Hill, New York*. [10] Ita, J. & Stixrude, L. (1992) *JGR* 97, 6849–6866. [11] Katsura, T. & Ito, E (1989) *JGR* 94, 15663–15670. [12] Fei, Y. & Bertka, C. M. (1999) *In Mantle Petrology: Field Observations and High-Pressure Experimentation: A Tribute to F. R. Boyd*. [13] Chen, J. et al. (2002) *GRL* 29, 1875 (2002). [14] Smyth, J. R. & Frost, D. J (2002) *GRL* 29, 123-1-123–4. [15] InSight Mars SEIS Data Service (2019). SEIS raw data, Insight Mission. [16] Clinton, J. F. *et al.* (2021) *Phys. of the Earth & Planet. Interiors* 310, 106595. [17] Montalbetti, J. F. & Kanasewich, E. R. (1970) *Geophysical Journal of the Royal Astronomical Society* 21, 119–129. [18] Rivoldini, A. *et al.* (2011), Icarus, 213, 451-472; [19] Nissen-Meyer, T. *et al.* (2014) *Solid Earth* 5, 425–445; [20] Khan, A. *et al.* (2021) *Science* 373, 434–438. [21] Baratoux, D. *et al.* (2011) *Nature* 472, 338–341. [22] Samuel, H. *et al.* (2019) *Nature* 569, 523–527. [23] Plesa, A.-C. *et al.* (2018) *GRL* 45, 2580-2589.